Electronic Supplementary Material (ESI) for ChemComm.

Supplementary Information

Guest-Selective and Reversible Magnetic Phase Switching in a Pseudo-Pillared-Layer Porous Magnet

Haruka Yoshino,[a] Narumi Tomokage,[a] Akio Mishima,[a] Benjamin Le Ouay,[a] Ryo Ohtani,[a] Wataru Kosaka,[bc] Hitoshi Miyasaka[bc] and Masaaki Ohba*[a]

[a] *Department of Chemistry, Graduate School of Science, Kyushu University, Motooka 744, Nishi-ku, Fukuoka 819-0395, Japan. E-mail: ohba@chem.kyushu-univ.jp*

[b] *Institute for Materials Research, Tohoku University, 2-1-1 Katahira, Aoba-ku, Sendai 980-8577, Japan*

[c] *Department of Chemistry, Graduate School of Science, Tohoku University, 6-3 Aramaki-Aza-Aoba, Aoba-ku, Sendai 980-8578, Japan*

Physical Measurement

Elemental analysis of carbon, hydrogen and nitrogen for $[Ni^{II}(dmen)_2]_2[Fe^{III}(CN)_6](AQDS)_{0.5}\cdot 7H_2O$ (**1_H$_2$O**; dmen = 1,1-dimethylethylenediamine, $AQDS^{2-}$ = 1,5-anthraquinonedisulfonate) was carried out at the division of graduate school of science in Kyushu University. Infrared (IR) spectra were recorded with a JASCO FT/IR-4200 spectrophotometer with an ATR accessory. Thermal gravimetric analysis (TGA) was performed using a Perkin Elmer STA6000 instrument, in the temperature range of 30–700°C, under N_2 atmosphere (heating rate: 5°C min^{-1}). PXRD patterns were collected on a Rigaku Ultima IV spectrometer. *In situ* PXRD measurement for dehydrated **1** was conducted under vacuum with a glass capillary connected to a homemade adsorption equipment. Adsorption and desorption isotherms were acquired using a BELSORP-MAX volumetric adsorption equipment (Microtrac BEL Corp.). The samples were dehydrated by heating at 400 K for 6 h before the measurements. The magnetic properties were investigated using a Quantum Design MPMS-XL5R SQUID. The samples were put into a gelatin capsule, placed in a plastic straw, and then fixed to the end of the sample transport rod. Diamagnetic correction was calculated by using Pascal constant.[1] The molar magnetic susceptibility (χ_M = *M/H*) were corrected for the diamagnetism of the constituent atoms and the sample tube. The temperature dependence of field cooled magnetization (FCM) curves were measured in the temperature range of 2–30 K under an applied magnetic field of 10 Oe. The field-dependence of magnetization curves were measured in the field range of -5 T to 5 T at 2 K. Temperature dependence of alternating–current (ac) magnetic susceptibilities (χ'_M = in phase, χ''_M = out of phase) were measured in the frequency range of 1–100 Hz under a zero dc field and an oscillating field of 3 Oe.

Single-crystal X-ray diffraction

Single-crystal X-ray diffraction data of **1_H$_2$O** were collected on a Bulker SMART APEX II ULTRA CCD-detector Diffractometer, a rotating-anode (Bruker Tourbo X-ray source) with graphite-monochromated $Mo_{K\alpha}$ radiation (λ = 0.71073 Å) was used. Computations were carried out on APEX2 crystallographic software package and OLEX2 software.[2] A single crystal was mounted on a polymer film with liquid paraffin and the

temperature kept constant under flowing N_2 gas. The structure of **1_H_2O** was solved by a standard direct method (XSHELL V6.3.1 crystallographic software package of the Bruker AXS) and expanded Fourier techniques. Full-matrix least-squares refinements were carried out with anisotropic thermal parameters for all non-disordered and non-hydrogen atoms. All of the hydrogen atoms were placed in the measured positions and refined using a riding model. Relevant crystal data collection and refinement data for the crystal structure of **1_H_2O** are summarized in Table S1. CCDC 2063060

Preparations

All chemicals were purchased from commercial sources and used without further purification. Precursor complex, $[Ni(dmen)_3]Cl_2$ (dmen = 1,1-dimethylethylenediamine, $H_2NC(CH_3)_2CH_2NH_2$) was prepared according to literature method.[3] $[Ni(dmen)_2]_2[Fe(CN)_6](AQDS)_{0.5}\cdot 7H_2O$ (**1_H_2O**; $AQDS^{2-}$ = 1,5-anthraquinonedisulfonate) was prepared by following steps.

Single Crystals of $[Ni^{II}(dmen)_2]_2[Fe^{III}(CN)_6](AQDS)_{0.5}\cdot 7H_2O$ (1_H_2O)

1_H_2O was prepared by a liquid phase diffusion method in a straight tube. A solution of $[Ni(dmen)_3]Cl_2$ (40 mg, 0.1 mmol) and Na_2AQDS (10.3 mg, 0.025 mmol) in H_2O (10 mL) were added to a solution of $K_3[Fe(CN)_6]$ (16 mg, 0.05 mmol) in H_2O (10 mL) at room temperature. The solution was allowed to stand for several weeks and the brown crystals were obtained. Yield: 72 %. Elemental analysis (%); Calcd. for $C_{29}H_{45}N_{14}SO_{9.5}Ni_2Fe$: C 36.24, H 6.19, N 20.40; found: C 36.25, H 6.42, N 20.45.

Powder Samples of 1

The dehydrated powder samples of **1** were prepared by heating **1_H_2O** under vacuum at 400 K for 6 h.

Powder Samples of 1_MeOH

The powder samples of methanol clathrate (**1_MeOH**) were prepared via a vapor diffusion method. The dehydrated powder samples of **1** were placed under MeOH vapor for 3 h.

Table S1. Crystallographic data and refinement parameter for **1_H_2O**

	1_H_2O CCDC 2063060
Formula	$C_{29}H_{48}N_{14}SO_{11}Ni_2Fe$
Temperature / K	100
Crystal system	Monoclinic
Space group	$P2_1/n$
a / Å	14.205(2)
b / Å	21.812(2)
c / Å	14.694(2)
α / °	90
β / °	90.464(1)
γ / °	90
V / Å^3	4552.7(8)
Z	4
GOF	1.046
R_1	4.57
wR_2	13.2

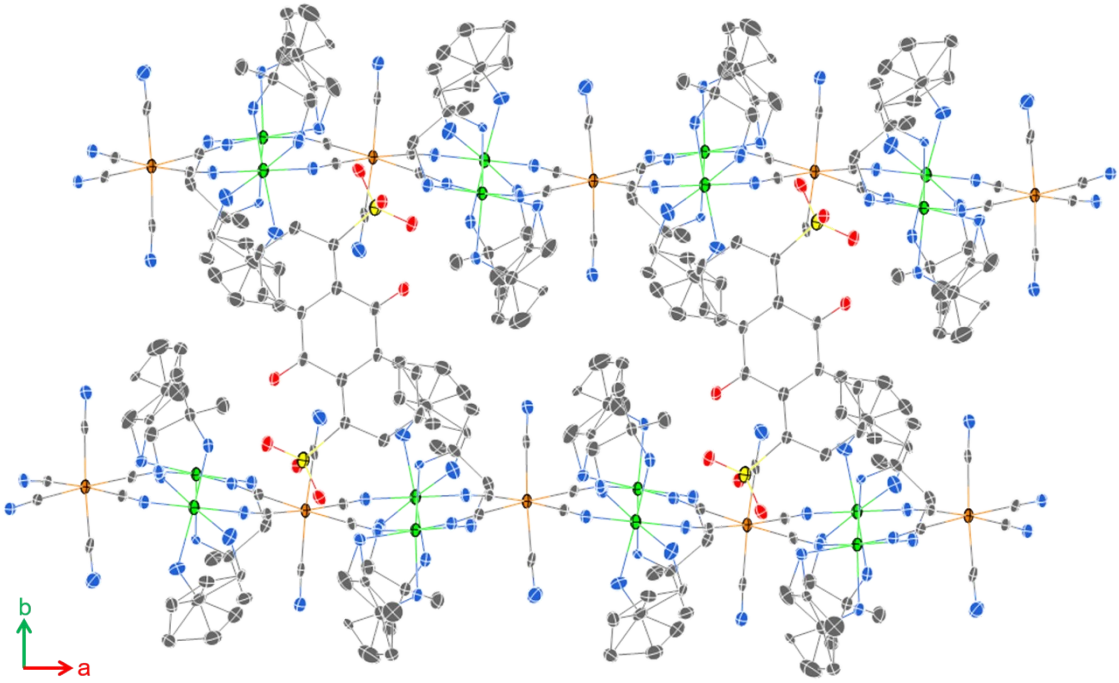

Fig. S1 An ORTEP drawing of the crystal structure for **1_H_2O** from a view along c-axis. Atomic code: Fe, orange; Ni, green; C, grey; N, blue; O, red; S, yellow, respectively. Lattice solvents and H atoms are omitted for clarity. Thermal ellipsoids are shown at the 50% probability level.

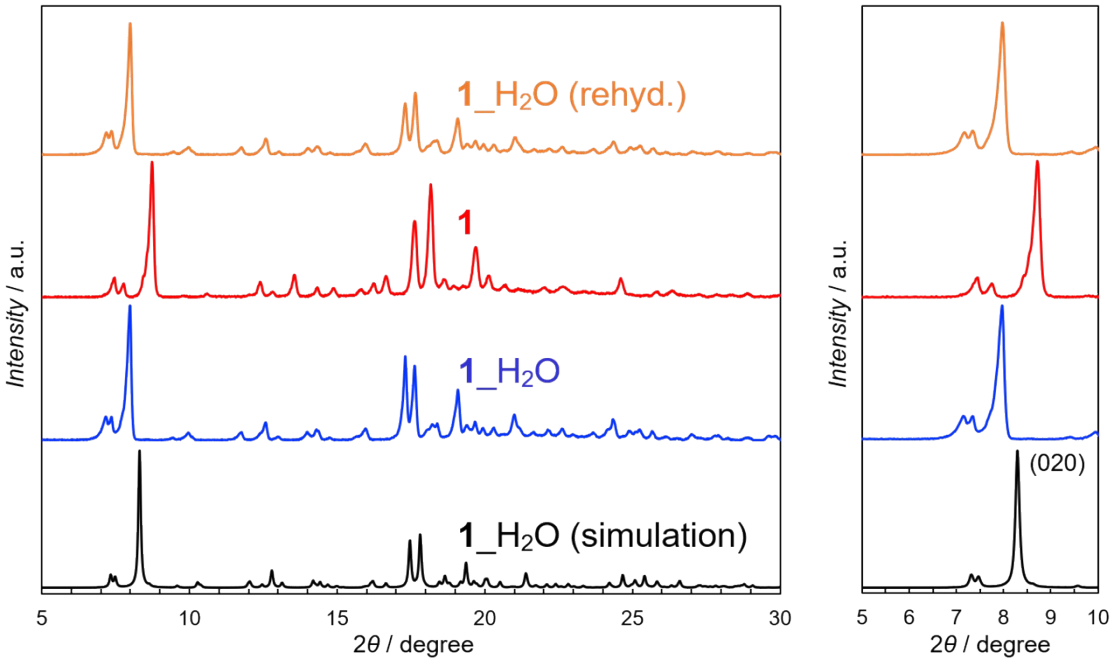

Fig. S2 PXRD patterns of **1_H_2O** (blue), **1** (red), **1_H_2O** (rehyd.) (orange) and simulated pattern of **1_H_2O** (black)

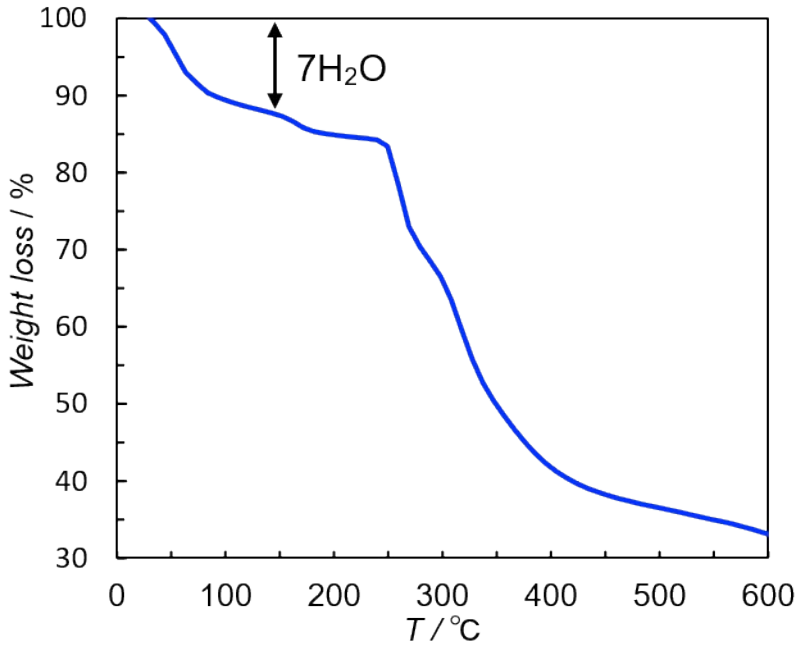

Fig. S3 TGA curve of **1_H_2O**

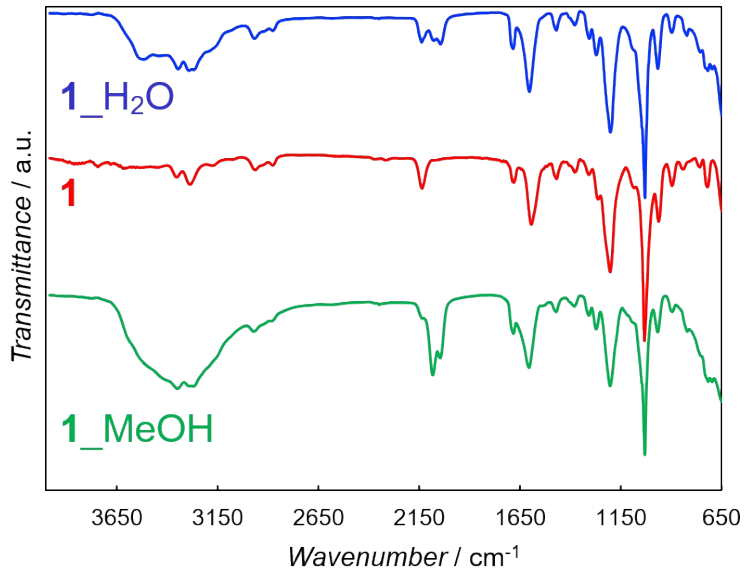

Fig. S4 IR spectra of (a) **1_H_2O** (blue), **1** (red), **1_MeOH** (green)

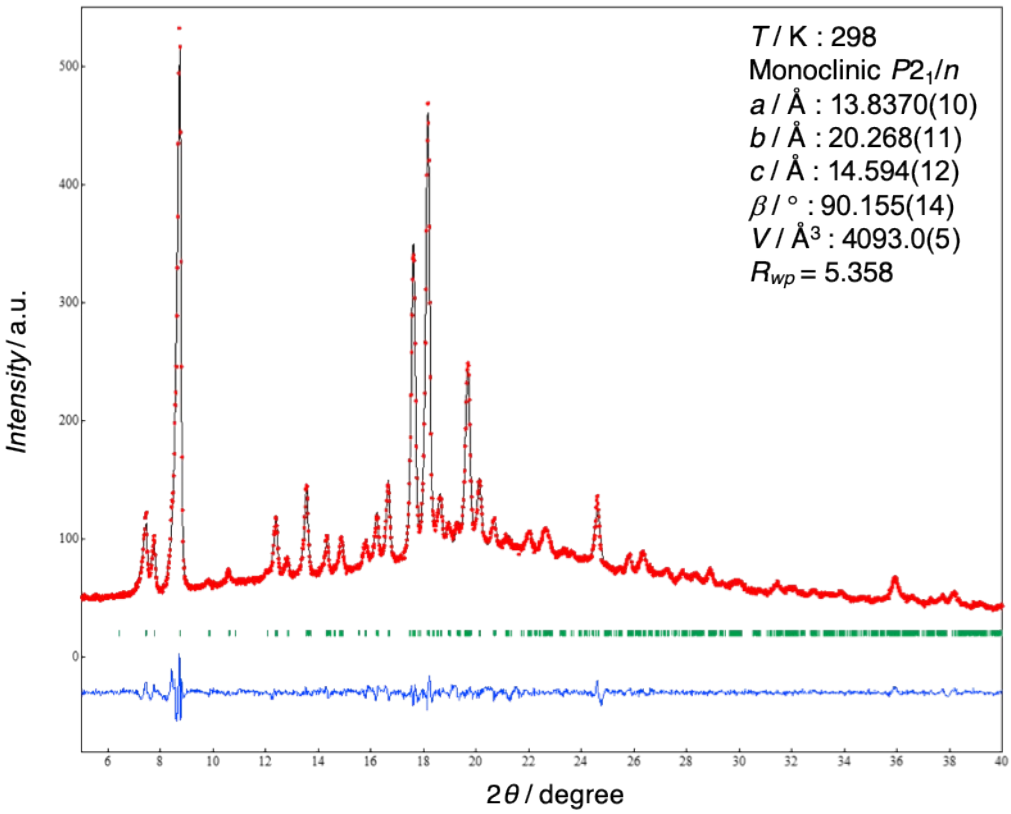

Fig. S5 Le Bail analysis of **1** under vacuum at 298 K with the results of PXRD pattern (λ = 1.5418 Å). Red dots, black line, and blue line represent the observed plots, calculated pattern, and their difference, respectively. Green bars are the calculated positions of the Bragg reflections.

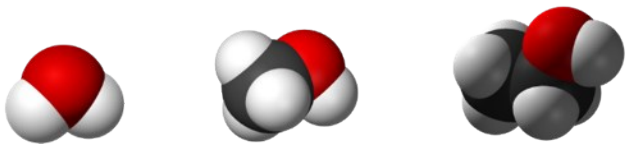

	H_2O	MeOH	EtOH
Kinetic diameter (Å)	2.641	3.626	4.530

Fig. S6 Kinetic diameter of H_2O, MeOH and EtOH[4]

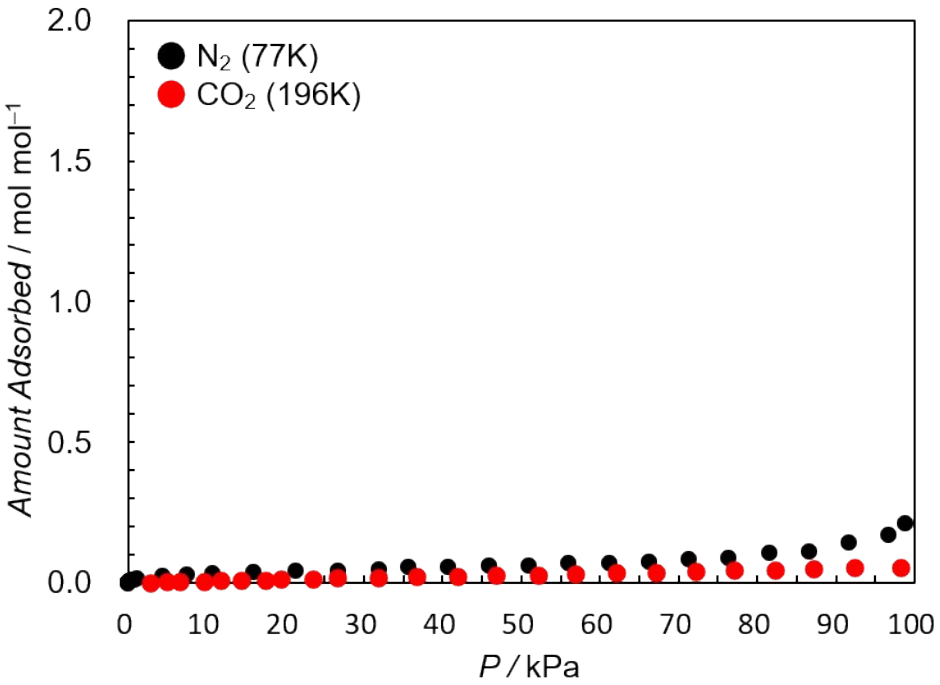

Fig. S7 Adsorption isotherms of **1** for N_2 (black) and CO_2 (red). The filled circles display the adsorption process.

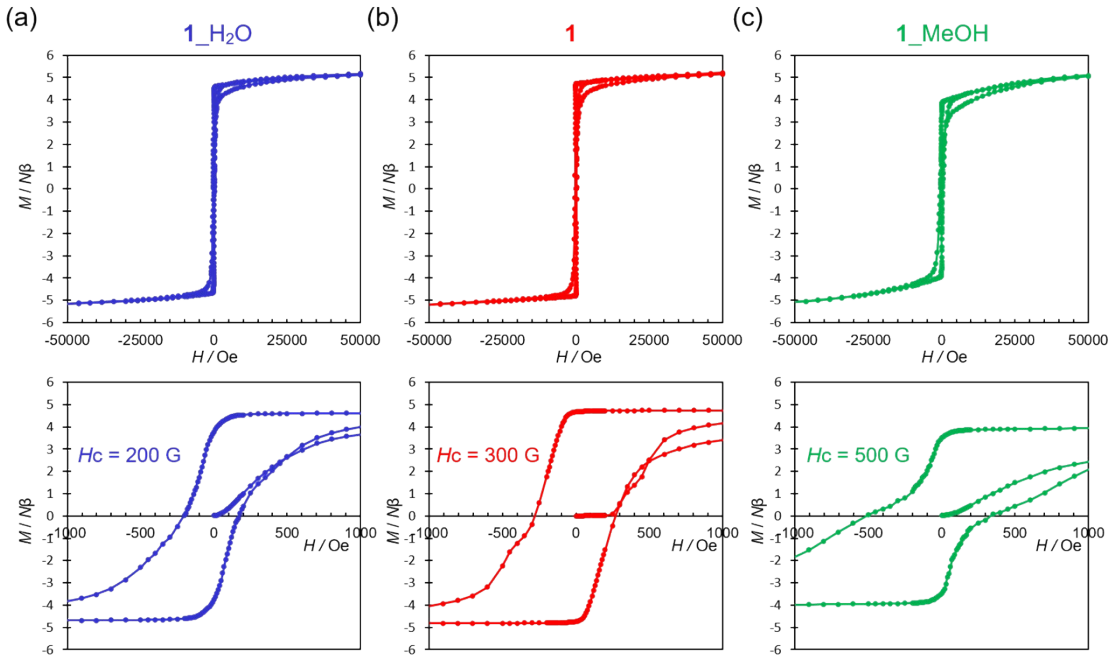

Fig. S8 Magnetic hysteresis curves of for (a) **1_H_2O** (blue), (b) **1** (red) and (c) **1_MeOH** (green) at 2 K.

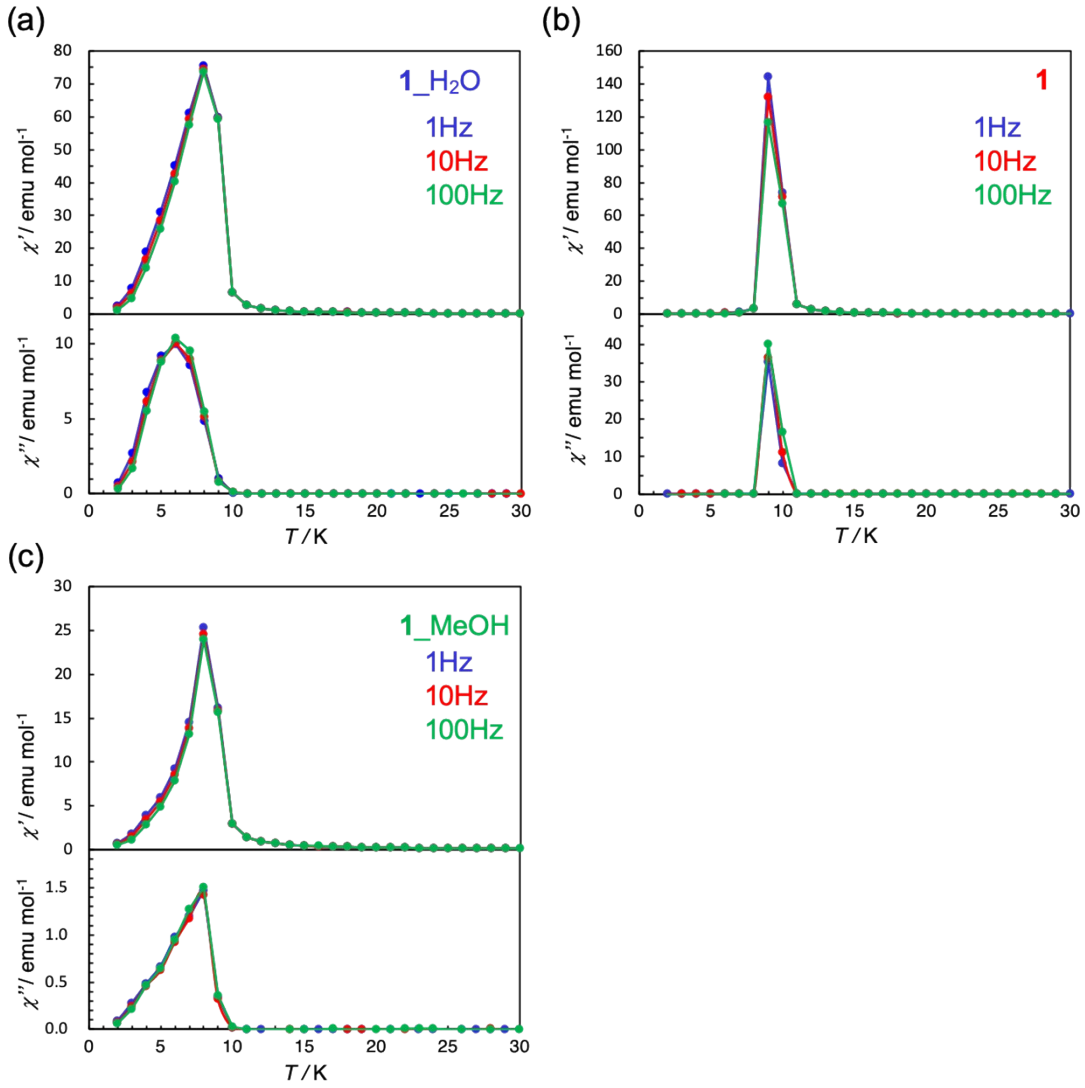

Fig. S9 Temperature dependence of χ'_M *vs*. *T* and χ''_M *vs*. *T* plots for (a) **1_H$_2$O**, (b) **1** and (c) **1_MeOH** measured in the frequency range of 1–100 Hz under a zero dc field and an oscillating field of 3 Oe (temperature range: 2–30 K).

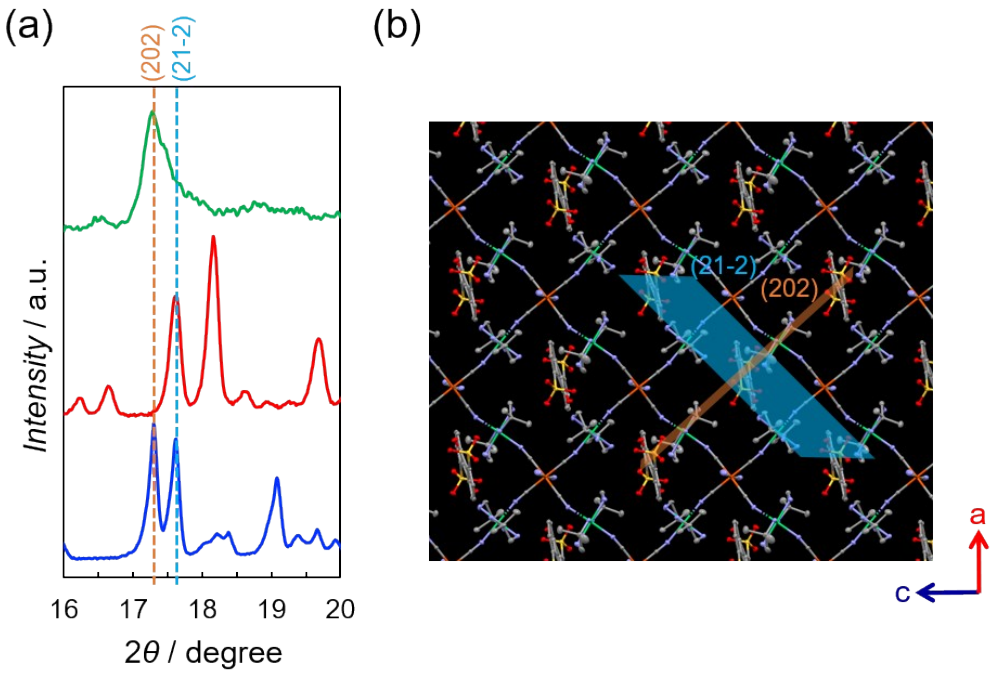

Fig. S10 (a) PXRD patterns of **1_H_2O** (blue), **1** (red) and **1_MeOH** (green). (b) Lattice plane of (202) and (21-2)

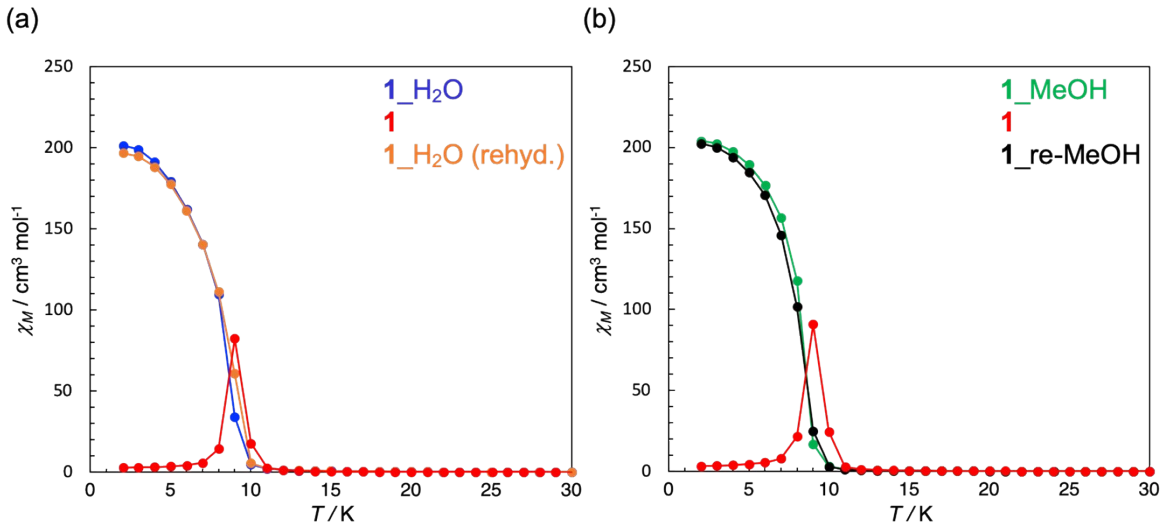

Fig. S11 Temperature dependence of χ_M *vs* *T* plots for (a) **1_H_2O** (blue), **1** (red), **1_H_2O** (rehyd.) (orange) and (b) **1_MeOH** (green), **1** (red), **1_re-MeOH** (black) under an applied magnetic field of 10 Oe.

Reference

1 Boudreaux, E. A. & Mulay, L. N. *Theory and Applications of Molecular Paramagnetism.* (John Wiley & Sons, New York, 1976).

2 O. V. Dolomanov, L. J. Bourhis, R. J. Gildea, J. a. K. Howard and H. Puschmann, *J. Appl. Crystallogr.*, 2009, **42**, 339–341.

3 M. Ohba and H. Ōkawa, *Coord. Chem. Rev.*, 2000, 198, 313–328.

4 J. R. Li, R. J. Kuppler and H. C. Zhou, *Chem. Soc. Rev*., 2009, **38**, 1477–1504.